

Generative Tertiary Structure-based RNA Design

Cheng Tan^{*1,2} Zhangyang Gao^{*1,2} Stan Z. Li²

Abstract

Learning from 3D biological macromolecules with artificial intelligence technologies has been an emerging area. Computational protein design, known as the inverse of protein structure prediction, aims to generate protein sequences that will fold into the defined structure. Analogous to protein design, RNA design is also an important topic in synthetic biology, which aims to generate RNA sequences by given structures. However, existing RNA design methods mainly focus on the secondary structure, ignoring the informative tertiary structure, which is commonly used in protein design. To explore the complex coupling between RNA sequence and 3D structure, we introduce an RNA tertiary structure modeling method to efficiently capture useful information from the 3D structure of RNA. For a fair comparison, we collect abundant RNA data and split the data according to tertiary structures. With the standard dataset, we conduct a benchmark by employing structure-based protein design approaches with our RNA tertiary structure modeling method. We believe our work will stimulate the future development of tertiary structure-based RNA design and bridge the gap between the RNA 3D structures and sequences. The code and benchmark dataset will be released.

1. Introduction

Ribonucleic acid (RNA) is essential in structural biology for its diverse functional classes (Crick, 1970; Noller, 1984; Rich & RajBhandary, 1976; Geisler & Coller, 2013). Recent research has revealed that functional non-coding RNA molecules, which are not translated into proteins, play a vital role in regulatory processes and transcription control (Runge et al., 2018; Feingold & Pachter, 2004; Gstyr

^{*}Equal contribution ¹Zhejiang University ²AI Research and Innovation Lab, Westlake University. Correspondence to: Stan Z. Li <Stan.ZQ.Li@westlake.edu.cn>, Cheng Tan <tancheng@westlake.edu.cn>.

et al., 2014; Kaushik et al., 2018). Functional RNAs (Vandivier et al., 2016) can modulate epigenetic marks (Law & Jacobsen, 2010), alter mRNA stability and translation (Roth & Breaker, 2009), regulate alternative splicing (Wanrooij et al., 2010), transduce signals (Kortmann & Narberhaus, 2012), and scaffold large macromolecular complexes (Ramakrishnan, 2014). The specific functions of an RNA molecule are determined by its structure (Sloma & Mathews, 2016). Therefore, exploring the intrinsic structural properties of RNA and revealing the connection between the RNA structure and sequence are of growing significance in medicine and synthetic biology (Delebecque et al., 2011; 2012; Guo et al., 2010; Meyer et al., 2016; Dotu et al., 2014; Wachsmuth et al., 2013). We show the schematic diagrams of RNA primary, secondary, tertiary structures in Figure 1.

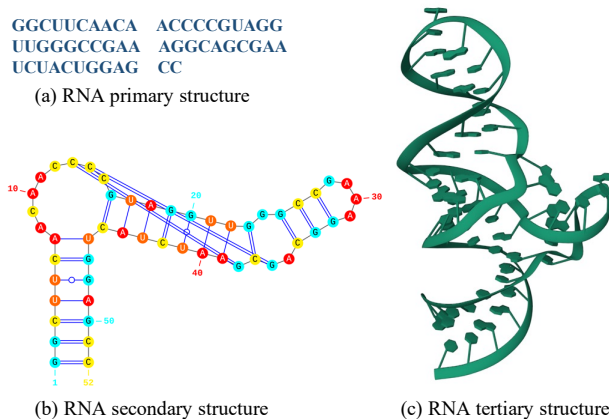


Figure 1. The schematic diagrams of RNA primary, secondary and tertiary structures, taking PDB 6TB7 as an example.

Recent years have witnessed the emergence of deep learning (Tan et al., 2021; 2022e; Gao et al., 2022e; Cao et al., 2022; Tan et al., 2022a;c; Zheng et al., 2022; Gao et al., 2021) and elegant computational RNA engineering (Jacobson & Zuker, 1993; McCaskill, 1990; Mathews et al., 2004; Hofacker, 2009; Zadeh et al., 2011a; Xiong et al., 2021; Singh et al., 2021). In particular, RNA folding algorithms have been extensively developed and expanded over the past several years, yielding a series of impressive works on RNA secondary structure prediction using a large amount of secondary structure data (Singh et al., 2019; Chen et al., 2019b;

Fu et al., 2022; Tan et al., 2022b). However, the knowledge of RNA 3D structures which is extremely important for a comprehensive understanding of the RNA functional mechanisms and discovering RNA-targeted drugs (Warner et al., 2018; Churkin et al., 2018), is not well explored (Townshend et al., 2021). AlphaFold2 (Jumper et al., 2021), one of the most revolutionary breakthroughs of AI in science, can predict tertiary protein structures with high accuracy. The progress of protein structure prediction (Jumper et al., 2021; Baek et al., 2021) inspires researchers to turn their attention to an even more challenging problem, RNA tertiary structure prediction, thus emerging 3D RNA folding algorithms such as DeepFoldRNA (Pearce et al., 2022), RoseTTAFoldNA (Baek et al., 2022), RhoFold (Chen et al., 2022; Shen et al., 2022).

Though promising, the knowledge of RNA tertiary structures lags far behind that of protein tertiary structures (Townshend et al., 2021): the proportion of the human genome transcribed to RNA is about 30 times higher than that coding for proteins (Bernstein et al., 2012), but the number of available RNA structures is less than 1% of that for proteins (Berman et al., 2000). How to efficiently take advantage of a small amount of data becomes a core issue in tertiary structure-based RNA engineering. While RNA 3D structure prediction can leverage pre-trained language models learned from a mass of RNA sequence data (Chen et al., 2022), its inverse problem, tertiary structure-based RNA design, is much more thorny. Existing works mainly focus on secondary structure-based RNA design (Hofacker et al., 1994; Dirks et al., 2004; Zadeh et al., 2011b; Garcia-Martin et al., 2013; 2015; Kleinkauf et al., 2015a;b; Retwitzer et al., 2020), which aims to design optimized RNAs with favorable properties by given secondary structures.

Compared to secondary structure-based RNA design, tertiary structure-based RNA design has fewer data but more complete structural information. In this work, we aim to directly explore the inherent structure-to-sequence relationships of RNA. Our main contributions can be summarized as follow:

- There are many homologous data in existing RNA 3D structures from PDB (Berman et al., 2000). To build a fair benchmark and avoid data bias, we collect massive pairs of RNA sequences and 3D structures and strictly split them according to their structural similarities rather than sequence similarities.
- We introduce an RNA tertiary structure modeling method to capture valuable information from the 3D structure of RNA. Motivate by the recent progress in structure-based protein design (Cao et al., 2021; Ingraham et al., 2019; Tan et al., 2022f; Jing et al., 2020; Strokach et al., 2020; Gao et al., 2022a;b; Hsu et al.,

2022; Dauparas et al., 2022), we represent the RNA molecules as a graph over the atom level and extract rotational and translational invariant features efficiently.

- We build a tertiary structure-based benchmark by employing several protein design approaches with our RNA 3D structure modeling method. We believe this benchmark will assist researchers in understanding RNA molecules from a novel perspective.

2. Related Work

2.1. Biomolecular Engineering

Biomolecular engineering is an emerging research field at the interface of molecular biology, biophysical chemistry, and chemical engineering (Nagamune, 2017; Gao et al., 2022c;d). Aiming to develop novel molecules, the primary goal of such research is to translate the understanding of the fundamental principles of physical biochemistry into useful processes that will benefit human health (Ryu & Nam, 2000). It has a wide range of applications (Pugh et al., 2018), e.g., new enzymes for industrial biocatalysis (Jeschek et al., 2016), highly tailored antibodies for cancer treatment (Rosenbaum, 2017), easily trackable fluorescent proteins for biological research (Martell et al., 2016) and efficient polymerases for forensic DNA detection (Ellefson et al., 2016). Protein/RNA design can be regarded as a kind of biomolecular engineering. Moreover, the structure prediction of biomolecules (Jumper et al., 2021; Baek et al., 2021; 2022; Pearce et al., 2022) also plays an important role in understanding the relationship between their structures, functions, and sequences towards purposely manipulating proteins and nucleic acids. In this work, we mainly focus on the structure-to-sequence biomolecular design task and typically aim at tertiary structure-based RNA design.

2.2. Protein Design

Benefitting from the abundant structure data, research on computational protein engineering has been of growing interest in recent years (Hu et al., 2022; Tan et al., 2022d). Early works employ multi-layer perceptron (MLP) to predict the type of each residue in the protein sequence, which focuses on feature extraction from protein 3D structure. SPIN (Li et al., 2014) integrates torsion angles (ϕ and ψ), fragment-derived sequence profiles, and structure-derived energy profiles to predict protein sequences. SPIN2 (O’Connell et al., 2018) introduces backbone angles (θ and τ), local contact number, and neighborhood distance. The subsequent work (Wang et al., 2018) further involves the solvent-accessible surface area of backbone atoms, secondary structure types, unit directions, and other related features. Convolutional neural networks (CNN) are also introduced in secondary structure-based protein de-

sign (Chen et al., 2019a), which prompts subsequent works on the tertiary structure-based protein design problem with 3D CNN such as ProDCoNN (Zhang et al., 2020) and DenseCPD (Qi & Zhang, 2020).

With the recent advances in graph neural networks, representing protein 3D structure by graph has been favored by a series of works. GraphTrans (Ingraham et al., 2019) is a seminal work on graph-based tertiary structure-based protein design, which combines attention (Vaswani et al., 2017) and auto-regressive decoding mechanisms to generate protein sequences. GVP (Jing et al., 2020) proposes the geometric vector perceptron, which learns both scalar and vector features in an equivariant and invariant manner concerning rotations and reflections. GCA (Tan et al., 2022f) introduces global and local graph attention to boost performance. ProteinMPNN (Dauparas et al., 2022) and ESM-IF (Hsu et al., 2022) reveal that more features and data can achieve dramatic improvements. AlphaDesign (Gao et al., 2022a) and PiFold (Gao et al., 2022b) also representative works that involves non-auto-regressive decoding strategies. Motivated by the outstanding performance of these graph-based models, we build the tertiary structure-based benchmark based on graph neural networks.

2.3. RNA Design

Introduced by Vienna (Hofacker et al., 1994), secondary structure-based RNA design have been extensively developed in the last decades. Early works solve the RNA design problem by stochastic optimization and performing energy minimization with thermodynamic parameters, e.g., RNAfold (Hofacker, 2003; Lorenz et al., 2011), Mfold (Zuker, 2003), UNAFold (Nicholas & Zuker, 2008), and RNAstructure (Mathews, 2014). Probabilistic models and posterior decoding are also employed in solving this problem. PFold (Knudsen & Hein, 2003) and CentroidFold (Sato et al., 2009) can be used when a seed RNA sequence is given. Local search strategies are performed to mutate the seed RNA sequence and apply repeatedly the direct problem of RNA folding prediction by energy minimization. In the vicinity of the seed RNA sequence, the designed sequence is searched out with desired folding properties according to the objective function in the optimization problem formulation (Churkin et al., 2018). The other works that operate on a single sequence and try to find a solution by changing a small number of nucleotides include RNAInverse (Hofacker et al., 1994), RNA-SSD (Andronescu et al., 2004), INFO-RNA (Busch & Backofen, 2006), and NUPACK (Zadeh et al., 2011a). There are also global searching methods, including antaRNA (Kleinkauf et al., 2015a) and MCTS-RNA (Yang et al., 2017). Learning-based methods based on reinforcement learning are also developed in this field (Eastman et al., 2018; Runge et al., 2018).

Though the secondary structure-based RNA design problem is followed with great interest, the tertiary structure-based RNA design is not well explored. In this work, we aim to take the first step in building a fair and standard benchmark for tertiary structure-based RNA design.

3. Method

3.1. Preliminaries

The primary structure of RNA is the linear sequence of nucleotides, typically notated as a string of letters. An RNA sequence $\mathcal{S}^N = \{(a)^N | a \in \{A, U, C, G\}\}$ has N nucleotide bases while each of them is represented by a letter of four possible letters such as A (*Adenine*), U (*Uracil*), C (*Cytosine*), G (*Guanine*). The sequence of non-coding RNA can fold into an RNA tertiary structure $\mathcal{X}^N = \{\mathbf{x}_i^\omega \in \mathbb{R}^3 : 1 \leq i \leq N, i \in \mathbb{R}^{N+} | \omega \in \{P, O5', C5', C4', C3', O3'\}\}$, where N is the number of nucleotides and ω indicates the atom in RNA. Here we consider the six main chains. The tertiary structure-based RNA design problem can be formally represented as:

$$\mathcal{F}_\Theta : \mathcal{X}^N \mapsto \mathcal{S}^N. \quad (1)$$

where \mathcal{F}_Θ is a learnable mapping with parameters Θ which is implemented by graph neural networks in our work.

3.2. Benchmark Dataset Construction

To build a fair benchmark, we collect all the RNA structures and corresponding sequences at better than 4.0 Å from PDB (Rose et al., 2016). All the collected structures were split into individual chains. Previous works on RNA tertiary structure prediction (Baek et al., 2022; Pearce et al., 2022; Shen et al., 2022) usually apply sequence similarity to cluster the data because these works start from sequences and predict corresponding structures. RNA design, in contrast, starts from structures and predicts corresponding sequences. Thus, we calculate the structural similarities by using RNA-align (Gong et al., 2019), which is a size-independent and statistically interpretable scoring metric based on TM-score (Zhang & Skolnick, 2004; 2005). The training, validation, and testing sets are split according to the structural similarities that ensure there are no samples that have similarities over 0.45 in each set. Eventually, we assembled a comprehensive dataset that includes a training set with 525 samples, a validation set with 74 samples, and a testing set with 29 samples. The data is strictly split by the tertiary structure and thus avoids the possible bias of homologous information.

3.3. Graph-based Tertiary Structure modeling

Extracting the key features with rotational and translational invariant properties is important for an efficient graph-based

tertiary structure-based RNA design. Motivated by the graph-based protein design approaches (Ingraham et al., 2019; Gao et al., 2022a;b), we first represent an RNA tertiary structure as an attributed graph and then construct rotational and translational invariant features in node embedding and edge embedding.

Representing tertiary structure as graph We represent RNA tertiary structure in terms of an attributed graph $\mathcal{G} = (V, E)$ with node features V and edge features E . The graph is constructed by building k -nearest neighbors in 3D space and there is a set of neighbors $\mathcal{N}(i, K)$ with k neighbors for each node i . Specifically, $V \in \mathbb{R}^{N \times f_n}$ contains node features of f_n dimensions for N nodes, and $E \in \mathbb{R}^{K \times f_m}$ contains edge features of f_m dimensions for K neighbors. Empirically, we set $k = 30$ in default.

Building local coordinate system We extract rotational and translational invariant features from the tertiary structure of RNA. For each nucleotide, we first build a local coordinate system defined as:

$$\mathbf{Q}_i = [\mathbf{b}_i, \mathbf{n}_i, \mathbf{b}_i \times \mathbf{n}_i], \quad (2)$$

where \mathbf{b}_i is the negative bisector of angles between the rays of contiguous coordinates $(\mathbf{x}_{i-1}, \mathbf{x}_i)$ and $(\mathbf{x}_i, \mathbf{x}_{i+1})$, and \mathbf{n}_i is a unit vector normal to that plane. In detail, \mathbf{b}_i and \mathbf{n}_i can be formally represented as:

$$\mathbf{u}_i = \frac{\mathbf{x}_i - \mathbf{x}_{i-1}}{\|\mathbf{x}_i - \mathbf{x}_{i-1}\|}, \mathbf{b}_i = \frac{\mathbf{u}_i - \mathbf{u}_{i+1}}{\|\mathbf{u}_i - \mathbf{u}_{i+1}\|}, \mathbf{n}_i = \frac{\mathbf{u}_i \times \mathbf{u}_{i+1}}{\|\mathbf{u}_i \times \mathbf{u}_{i+1}\|}. \quad (3)$$

The process of building the local coordinate system can be visualized, as shown in Figure 2. As the local coordinate system relies on a fixed set for a specific atom, it is tolerant to arbitrary rotations and translations.

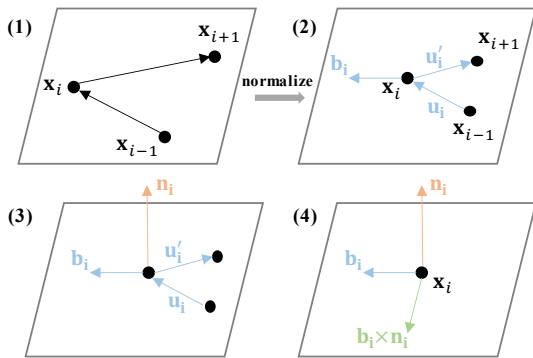


Figure 2. The steps of building a local coordinate system.

Constructing node features The node features consist of three aspects: (1) Angle features, the sin and cos embeddings of six backbone torsion angles. The backbone of the RNA tertiary structure consists of a repeating unit

of six single bonds. The six backbone torsion angles are rotations about bonds $P_i - O5'_i(\alpha)$, $O5'_i - C5'_i(\beta)$, $C5'_i - C4'_i(\gamma)$, $C4'_i - C3'_i(\delta)$, $C3'_i - O3'_i(\epsilon)$, $O3'_i - P_{i+1}(\zeta)$. Formally, the angle features of RNA tertiary structures can be represented as:

$$\{\sin, \cos\} \times \{\alpha_i, \beta_i, \gamma_i, \delta_i, \epsilon_i, \zeta_i\}. \quad (4)$$

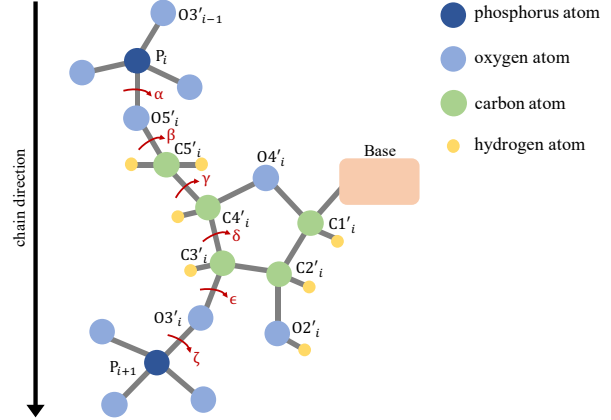


Figure 3. An example illustration of nucleotide structures in an RNA. We denote the six main chain torsion angles with red arrows, i.e., $\alpha, \beta, \gamma, \delta, \epsilon, \zeta$.

(2) Intra-nucleotide distance features, distance encodings of spatial distances between the other intra-nucleotide atoms and the atom $C3'_i$ lifted into radial basis. The node distance features can be formally written as:

$$\{\text{RBF}(\|\omega_i - C3'_i\|) \mid \omega \in \{P, O5', C5', C4', O3'\}\}. \quad (5)$$

(3) Intra-nucleotide direction features, the directions of the other intra-nucleotide atoms to the atom $C3'_i$. Here, we leverage the local coordinate system \mathbf{Q}_i of the i -th atom $C3'_i$ to connect this atom to the other atoms in the nucleotide by their directions. The node direction features can be represented as:

$$\left\{ \mathbf{Q}_i^T \frac{\omega_i - C3'_i}{\|\omega_i - C3'_i\|} \mid \omega \in \{P, O5', C5', C4', O3'\} \right\}. \quad (6)$$

Constructing edge features The edge features also consist of three aspects: (1) Orientation features, an orientation encoding $\mathbf{q}(\cdot)$ of the quaternion representation of the spatial rotation matrix $\mathbf{Q}_i^T \mathbf{Q}_j$. Each quaternion contains four scalar variables that can be used to efficiently represent the three-dimensional rotations. The orientation features are formally defined as:

$$\mathbf{q}(\mathbf{Q}_i^T \mathbf{Q}_j). \quad (7)$$

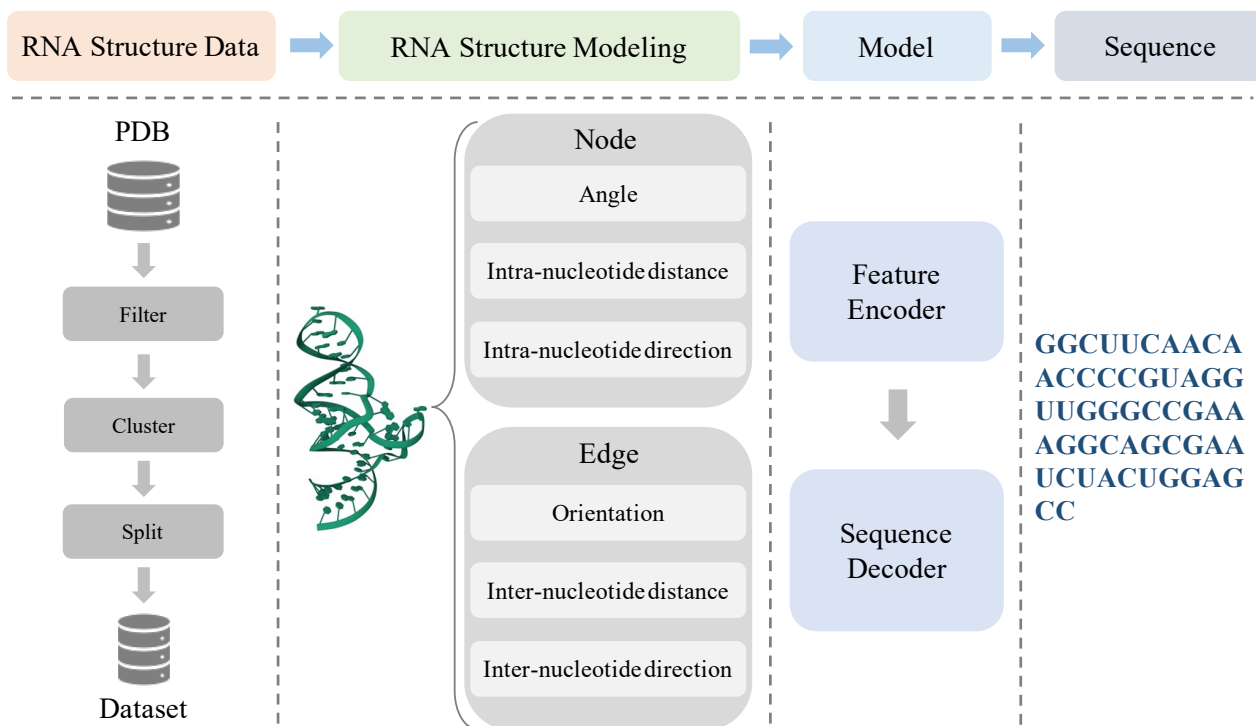


Figure 4. The overview of the tertiary structure-based RNA design pipeline. The pipeline can be divided into four steps: (i) dataset collection, (ii) structure modeling, (iii) model training, and (iv) sequence generation.

(2) Inter-nucleotide distance features, distance encodings of spatial distances between inter-nucleotide atoms from neighbor nucleotides and the atom $C3'_i$ lifted into radial basis. Though analogous to the node distance features, the edge distance features focus on the distances between atoms from different nucleotides. The edge distance features can be written as:

$$\left\{ \text{RBF}(\|\omega_j - C3'_i\|) \mid j \in \mathcal{N}(i, K), \right. \\ \left. \omega \in \{P, O5', C5', C4', O3'\} \right\}. \quad (8)$$

(3) Inter-nucleotide direction features, the directions of inter-nucleotide atoms to the atom $C3'_i$. Note that here we add the atoms $C3'_j$ from other nucleotides. The edge direction features are represented as:

$$\left\{ \mathbf{Q}_i^T \frac{\omega_j - C3'_i}{\|\omega_j - C3'_i\|} \mid j \in \mathcal{N}(i, K), \right. \\ \left. \omega \in \{P, O5', C5', C4', C3', O3'\} \right\}. \quad (9)$$

We present the overall framework of tertiary structure-based RNA design in Figure 4. This framework provides a strict data split pipeline for building a standard benchmark dataset. Moreover, a comprehensive tertiary structure modeling method is proposed by efficiently extracting expressive features. With the collected standard dataset and

the complete RNA structure modeling, we have extracted essential features from the RNA tertiary structures. The next step is to build baseline models based on those extracted features. Here, we recognize the RNA design as a structure-to-sequence translation problem, where structure features have been provided by the previous steps. We build baseline models by dividing the model into two parts, i.e., feature encoder and sequence decoder. The feature encoder learns from the features and outputs valuable representations and the sequence decoder decodes the representations into sequences. We leave the details in the experiment section.

4. Experiments

4.1. Benchmark Comparison

Metric Following (Li et al., 2014; O’Connell et al., 2018; Wang et al., 2018; Ingraham et al., 2019; Jing et al., 2020; Tan et al., 2022f; Gao et al., 2022a;b), we apply sequence perplexity and recovery as two important metrics in evaluating the model performance. Specifically, the perplexity is defined from a natural language perspective to evaluate whether the output sequence appears to be true. It can be

formally represented as:

$$\text{Perplexity}(\mathcal{S}^N, \mathcal{X}^N) = \exp\left(-\frac{1}{N} \sum_{i=1}^N \mathcal{S}_i^N \log p(\mathcal{S}_i^N | \mathcal{X})\right), \quad (10)$$

where \mathcal{S}_i^N is the i -th nucleotide in an RNA with total N nucleotides, and $p(\mathcal{S}_i^N | \mathcal{X})$ is the output probability from the learned model.

Recovery is defined as the predicting accuracy of the RNA sequence at the per-nucleotide level:

$$\text{Recovery}(\mathcal{S}^N, \mathcal{X}^N) = \frac{1}{N} \sum_{i=1}^N \mathbb{1}[\mathcal{S}_i^N = \arg \max p(\mathcal{S}_i^N | \mathcal{X})]. \quad (11)$$

Setting In all experiments, we train the model for 50 epochs using the Adam optimizer with a learning rate of 0.001. The batch size is set as 4 by default. The model is implemented based on the standard PyTorch Geometric (Fey & Lenssen, 2019) library using the PyTorch 1.11.0 library. We run the models on Intel(R) Xeon(R) Gold 6240R CPU @ 2.40GHz CPU and NVIDIA A100 GPU. Considering that the various length of RNA may have different effects on the prediction results, we roughly divide the testing set into three groups according to the length of RNA: (i) Short, RNA samples with a length less than or equal to 100; (ii) Medium, RNA samples with a length larger than 100 but less than or equal to 200; (iii) Long, RNA samples with a length larger than 200. The performance of baseline models on these groups of RNA samples is also considered an important issue for model generalization ability. The performance of baseline models on these groups of RNA samples is also considered an important issue for model generalization ability. Following (Ingraham et al., 2019; Jing et al., 2020; Tan et al., 2022f; Gao et al., 2022a), we report the mean recovery and the median recovery for each experiment.

Baseline As shown in Table 2, we include eight baseline models in our tertiary structure-based RNA design. These models can be divided into three categories: (i) sequential models that directly learn from RNA sequences unconditioned on structures, i.e., SeqRNN and SeqLSTM; (ii) multi-layer perceptron (MLP) models that learn from structure features while ignoring the graph structures, i.e., Structure MLP (SMLP); (iii) graph-based models that learn from node and edge features by neighbor graphs, i.e., Structure GNN (SGNN) and GraphTrans (GTrans). The first two categories provide a reference for graph-based models. Moreover, we also add non-auto-regressive (Non-AR) decoding versions for those structure-based models, with the prefix 'N-' in Table 2. The number of hidden units is set as 128, and the number of encoder and decoder layers is set as 3 by default. We also report the number of parameters and FLOPs by calculating a single sample with a length of 100.

Result We summarize the experimental results in Table 1. The recovery metrics of SeqRNN and SeqLSTM are not provided because they only generate verisimilar RNA sequences but cannot generate sequences conditioned on the structures. The overall perplexity metrics of SeqRNN and SeqLSTM are relatively worse than most of the other baseline models, but they obtain better perplexity on long RNA data. The possible reason may be other models conditioned on structures fail in long RNA design. It is worth noting that non-auto-regressive approaches usually have worse perplexity but better recovery. Considering the alphabet of the RNA design problem has only four characters (A, U, C, G), the perplexity metric which is defined from a natural language perspective may fail to accurately discriminate the quality of predicted RNA sequences. It can also be seen that N-StructGNN achieves the highest recovery score over all the RNA data, benefitting from its strong performance on short and medium samples. Though GraphTrans and N-GraphTrans require more parameters and larger computational resources than StructGNN and N-StructGNN, they are relatively worse in the recovery metric.

4.2. Generalization Assessment

To present a comprehensive comparison and assess the generalization ability of the baseline models, we report results on a dataset taken from the community-wide RNA-Puzzles experiment (Pearce et al., 2022; Cruz et al., 2012; Miao et al., 2015; 2017; 2020). Following DeepFoldRNA (Pearce et al., 2022), we collect the RNA-Puzzles dataset consisting of 17 non-redundant, monomeric RNA structures. We further calculate the structural similarities between the RNA-Puzzles dataset and our dataset by using RNA-align (Gong et al., 2019) and then remove samples that have similarities over 0.45 in the original RNA-Puzzles dataset. We finally obtain 12 non-redundant RNA sequence-structure pairs and evaluate the generalization ability of the baseline models pre-trained on our dataset. By testing on such an independent dataset, we can assess the generalization ability of baseline models with our proposed RNA tertiary structure modeling method.

We summarize the results on the non-overlapping independent RNA-Puzzles testing dataset in Table 4. It can be seen that the results on this dataset are consistent with those on the previous dataset, which indicates models trained on our standard dataset can actually learn the intrinsic connections between RNA sequences and tertiary structures and thus generalize to unseen data in practical applications. N-StructGNN achieves the highest recovery score among the baseline models and N-GraphTrans obtains the second highest. Consistent with the performance of the previous standard testing set, the perplexity metrics of N-StructGNN and N-GraphTrans are relatively worse than the other baseline models. Language models that are unconditioned on

Table 1. Experimental results on the standard dataset. Lower is better for perplexity, and higher is better for recovery. The **best** and suboptimal results are labeled with bold and underline.

Model	Perplexity (\downarrow)				Recovery (\uparrow)			
	Short	Medium	Long	All	Short	Medium	Long	All
SeqRNN	3.0889	2.8481	<u>2.2128</u>	3.5369	/	/	/	/
SeqLSTM	3.0014	2.7966	2.2089	3.5027	/	/	/	/
StructMLP	3.3287	3.4565	3.7123	3.3679	35.06	32.32	24.61	32.43
N-StructMLP	3.6511	3.7370	3.9852	3.6660	40.85	40.00	32.03	40.00
StructGNN	<u>2.3508</u>	<u>2.5825</u>	2.9601	<u>2.3719</u>	37.93	37.50	33.20	38.38
N-StructGNN	3.1815	3.4305	3.9625	3.2246	51.47	<u>51.60</u>	32.81	51.47
GraphTrans	2.3497	2.5324	3.0200	2.3582	40.00	34.23	35.94	36.84
N-GraphTrans	3.1437	3.3698	3.9306	3.1840	<u>49.02</u>	53.70	32.42	<u>49.73</u>

Table 2. An overview of baseline models. MPNN denotes message passing neural networks (Gilmer et al., 2017), and AR denotes the autoregressive decoding strategy.

	SeqRNN	SMLP	SGNN	GTrans
Encoder	RNN	MLP	MPNN	Transformer
Decoder	Non-AR	AR	AR	AR
Params (M)	0.199	1.366	1.366	2.106
FLOPs (G)	0.051	0.187	1.747	2.211

	SeqLSTM	N-SMLP	N-SGNN	N-GTrans
Encoder	LSTM	MLP	MPNN	Transformer
Decoder	Non-AR	Non-AR	Non-AR	Non-AR
Params (M)	0.794	1.317	1.317	2.008
FLOPs (G)	0.051	0.181	1.599	1.916

structures and other autoregressive models conditioned on structures usually have better perplexity. Still, we argue that the perplexity metric is not fully reliable in RNA design. The alphabet size of the output sequence is four, which is too small for the perplexity metric to accurately evaluate the predicted sequence quality. Thus, we consider the recovery score as a more reliable metric in our tertiary structure-based RNA design for its precise evaluation, which can be a reference for wet-lab experiments and practical applications.

4.3. Ablation on Features

The RNA tertiary structure modeling consists of various feature types. We naturally raise a problem: how much gain could be obtained from the introduced features? To investigate the importance of each feature, we conduct a comprehensive ablation study on the various feature types. The experimental setting of the feature ablation study is the same as it is in Section 4.1.

We summarize the results of the feature ablation in Table 3. It can be seen that angle features alone will result in significant performance degradation. The intra-nucleotide distance

and direction features can achieve comparable performance with the full features, while the distance features alone even unexpectedly achieve a bit higher recovery score, indicating the importance of intra-nucleotide distance features. For the edge features, the phenomenon is consistent with the node features, in which distance features alone achieve a higher recovery score than the other two feature types. We can also find that edge features play much more important roles than node features. We can also find that edge features play much more important roles than node features. If we use full edge features but part of node features, the recovery scores are 48.84, 51.72, and 51.11. In contrast, using full node features but part of edge features, the recovery scores are 39.68, 47.89, and 44.82. This phenomenon indicates the neighbors of nucleotides matter in learning RNA structure.

4.4. Invariance Analysis

For the RNA structures in three-dimensional space, the predicted output is supposed to be invariant to rotations and translations. The proposed RNA tertiary structure modeling method has constructed node and edge features based on the neighbor graph for each nucleotide. While rotations and translations cannot change the neighbor relationships of atoms, the rotational and translational invariance is guaranteed. However, there still exists floating point arithmetic errors in the computation of learning models, which may lead to different predicted outputs.

We analyze the invariance of baseline models by using the pre-trained models to infer the randomly rotated and translated testing data. The recovery scores are summarized in Table 5. It can be seen that the differences in recovery scores between the raw testing data and randomly rotated and translated testing data are minor for all baseline models with our tertiary structure modeling method, indicating the well-designed features can provide a basic guarantee for model invariance. Moreover, randomly rotating and translating the testing data does not change the ranks of baseline

Table 3. The results of ablation study on different features. Lower is better for perplexity, and higher is better for recovery. The checkmark means the corresponding feature is involved, and the blank means not involved.

Node	Angle	✓	✓			✓	✓	✓
	Distance	✓		✓		✓	✓	✓
	Direction	✓			✓	✓	✓	✓
Edge	Orientation	✓	✓	✓	✓	✓		
	Distance	✓	✓	✓	✓		✓	
	Direction	✓	✓	✓	✓			✓
Result	Perplexity (↓)	3.2246	3.2402	3.1311	3.1787	3.6551	3.2345	3.4811
	Recovery (↑)	51.47	48.84	51.72	51.11	39.68	47.89	44.82

Table 4. The results of generalization assessment on data from the RNA-Puzzles dataset. Lower is better for perplexity, and higher is better for recovery. The **best** and suboptimal results are labeled with bold and underline.

Model	Perplexity (↓)	Recovery (↑)
SeqRNN	2.5787	24.71
SeqLSTM	2.5319	24.36
StructMLP	3.5430	32.38
N-StructMLP	3.6686	37.20
StructGNN	2.4496	37.32
N-StructGNN	3.3250	48.83
GraphTrans	<u>2.4497</u>	35.65
N-GraphTrans	3.3558	<u>42.42</u>

models, i.e., N-StructGNN still takes the lead with the highest recovery score. The non-auto-regressive versions of models achieve lower differences after random rotation and translation, which suggests directly presenting nucleotide-level prediction is enough to achieve good performance.

Table 5. The recovery scores of inputting raw data and randomly rotated and translated data.

Model	Raw	Rotate+Translante	Difference
StructMLP	32.43	32.98	0.55
N-StructMLP	40.00	40.40	0.40
StructGNN	38.38	37.96	0.42
N-StructGNN	51.47	51.16	0.31
GraphTrans	36.84	36.21	0.63
N-GraphTrans	49.73	50.00	0.27

4.5. Visualization Examples

To show the effectiveness of designed sequences, we use the designed sequences to predict the structures of designed sequences and compare them with the ground truth structures. Here, we choose N-StructGNN as a baseline model to produce the sequences. The corresponding structures are predicted by a deep learning RNA tertiary structure prediction method, i.e., RhoFold (Shen et al., 2022). We show the

visualization examples in Figure 5.

It can be seen that the designed structures of 5KPY and 5TPY are similar to the ground truth structures. The other two designed structures share some similar substructures in part of structures. It is worth noting that the predictive accuracy of existing RNA 3D structure prediction models is inferior to AlphaFold2. The designed structures in our visualization examples may suffer from inaccurate structure predictions, which we provide here as a reference.

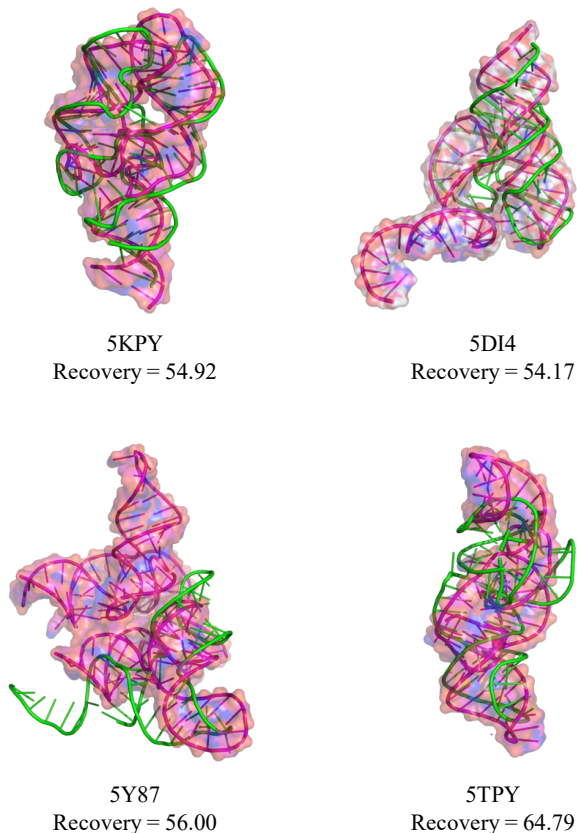


Figure 5. Examples of tertiary structure-based RNA design. We color the ground truth and the designed structures purple and green, respectively. The recovery scores are reported below.

5. Conclusion

In this study, we explore the tertiary structure-based RNA design, which aims to generate RNA sequences by given structures. We first assemble a benchmark dataset with abundant RNA data and split the data according to tertiary structures. To learn the complex coupling between RNA sequences and 3D structures, we propose an RNA tertiary structure modeling method by constructing nearest-neighbor graphs and capturing the atom-level node and edge features. Based on the standard dataset and the proposed structure modeling method, we build several baseline models for tertiary structure-based RNA design. We hope that our work can provide a new perspective on generative RNA design by introducing the tertiary structure.

References

- Andronescu, M., Fejes, A. P., Hutter, F., Hoos, H. H., and Condon, A. A new algorithm for rna secondary structure design. *Journal of molecular biology*, 336(3):607–624, 2004.
- Baek, M., DiMaio, F., Anishchenko, I., Dauparas, J., Ovchinnikov, S., Lee, G. R., Wang, J., Cong, Q., Kinch, L. N., Schaeffer, R. D., et al. Accurate prediction of protein structures and interactions using a three-track neural network. *Science*, 373(6557):871–876, 2021.
- Baek, M., McHugh, R., Anishchenko, I., Baker, D., and DiMaio, F. Accurate prediction of nucleic acid and protein-nucleic acid complexes using rosettafoldna. *bioRxiv*, 2022.
- Berman, H. M., Westbrook, J., Feng, Z., Gilliland, G., Bhat, T. N., Weissig, H., Shindyalov, I. N., and Bourne, P. E. The protein data bank. *Nucleic acids research*, 28(1):235–242, 2000.
- Bernstein, B., Birney, E., Dunham, I., Green, E., Gunter, C., and Snyder, M. Project consortium encode. *An integrated encyclopedia of DNA elements in the human genome. Nature*, 489:57–74, 2012.
- Busch, A. and Backofen, R. Info-rna—a fast approach to inverse rna folding. *Bioinformatics*, 22(15):1823–1831, 2006.
- Cao, H., Tan, C., Gao, Z., Chen, G., Heng, P.-A., and Li, S. Z. A survey on generative diffusion model. *arXiv preprint arXiv:2209.02646*, 2022.
- Cao, Y., Das, P., Chenthamarakshan, V., Chen, P.-Y., Melnyk, I., and Shen, Y. Fold2seq: A joint sequence (1d)-fold (3d) embedding-based generative model for protein design. In *International Conference on Machine Learning*, pp. 1261–1271. PMLR, 2021.
- Chen, J., Hu, Z., Sun, S., Tan, Q., Wang, Y., Yu, Q., Zong, L., Hong, L., Xiao, J., Shen, T., et al. Interpretable rna foundation model from unannotated data for highly accurate rna structure and function predictions. *bioRxiv*, 2022.
- Chen, S., Sun, Z., Lin, L., Liu, Z., Liu, X., Chong, Y., Lu, Y., Zhao, H., and Yang, Y. To improve protein sequence profile prediction through image captioning on pairwise residue distance map. *Journal of chemical information and modeling*, 60(1):391–399, 2019a.
- Chen, X., Li, Y., Umarov, R., Gao, X., and Song, L. Rna secondary structure prediction by learning unrolled algorithms. In *International Conference on Learning Representations*, 2019b.
- Churkin, A., Retwitzer, M. D., Reinharz, V., Ponty, Y., Waldispühl, J., and Barash, D. Design of rnas: comparing programs for inverse rna folding. *Briefings in bioinformatics*, 19(2):350–358, 2018.
- Crick, F. Central dogma of molecular biology. *Nature*, 227(5258):561–563, 1970.
- Cruz, J. A., Blanchet, M.-F., Boniecki, M., Bujnicki, J. M., Chen, S.-J., Cao, S., Das, R., Ding, F., Dokholyan, N. V., Flores, S. C., et al. Rna-puzzles: a casp-like evaluation of rna three-dimensional structure prediction. *Rna*, 18(4):610–625, 2012.
- Dauparas, J., Anishchenko, I., Bennett, N., Bai, H., Ragotte, R. J., Milles, L. F., Wicky, B. I., Courbet, A., de Haas, R. J., Bethel, N., et al. Robust deep learning-based protein sequence design using proteinmpnn. *Science*, 378(6615):49–56, 2022.
- Delebecque, C. J., Lindner, A. B., Silver, P. A., and Aldaye, F. A. Organization of intracellular reactions with rationally designed rna assemblies. *Science*, 333(6041):470–474, 2011.
- Delebecque, C. J., Silver, P. A., and Lindner, A. B. Designing and using rna scaffolds to assemble proteins in vivo. *Nature protocols*, 7(10):1797–1807, 2012.
- Dirks, R. M., Lin, M., Winfree, E., and Pierce, N. A. Paradigms for computational nucleic acid design. *Nucleic acids research*, 32(4):1392–1403, 2004.
- Dotu, I., Garcia-Martin, J. A., Slinger, B. L., Mechery, V., Meyer, M. M., and Clote, P. Complete rna inverse folding: computational design of functional hammerhead ribozymes. *Nucleic acids research*, 42(18):11752–11762, 2014.
- Eastman, P., Shi, J., Ramsundar, B., and Pande, V. S. Solving the rna design problem with reinforcement learning. *PLoS computational biology*, 14(6):e1006176, 2018.
- Ellefson, J. W., Gollihar, J., Shroff, R., Shivram, H., Iyer, V. R., and Ellington, A. D. Synthetic evolutionary origin of a proofreading reverse transcriptase. *Science*, 352(6293):1590–1593, 2016.
- Feingold, E. and Pachter, L. The encode (encyclopedia of dna elements) project. *Science*, 306(5696):636–640, 2004.
- Fey, M. and Lenssen, J. E. Fast graph representation learning with pytorch geometric. *arXiv preprint arXiv:1903.02428*, 2019.
- Fu, L., Cao, Y., Wu, J., Peng, Q., Nie, Q., and Xie, X. Ufold: fast and accurate rna secondary structure prediction with

- deep learning. *Nucleic acids research*, 50(3):e14–e14, 2022.
- Gao, Z., Lin, H., Tan, C., Wu, L., Li, S., et al. Git: Clustering based on graph of intensity topology. *arXiv preprint arXiv:2110.01274*, 2021.
- Gao, Z., Tan, C., Li, S., et al. Alphadesign: A graph protein design method and benchmark on alphafolddb. *arXiv preprint arXiv:2202.01079*, 2022a.
- Gao, Z., Tan, C., and Li, S. Z. Pifold: Toward effective and efficient protein inverse folding. *arXiv preprint arXiv:2209.12643*, 2022b.
- Gao, Z., Tan, C., Wu, L., and Li, S. Z. Cosp: Co-supervised pretraining of pocket and ligand. *arXiv preprint arXiv:2206.12241*, 2022c.
- Gao, Z., Tan, C., Wu, L., and Li, S. Z. Semiretro: Semi-template framework boosts deep retrosynthesis prediction. *arXiv preprint arXiv:2202.08205*, 2022d.
- Gao, Z., Tan, C., Wu, L., and Li, S. Z. Simvp: Simpler yet better video prediction. In *Proceedings of the IEEE/CVF Conference on Computer Vision and Pattern Recognition*, pp. 3170–3180, 2022e.
- Garcia-Martin, J. A., Clote, P., and Dotu, I. Rnaifold: a constraint programming algorithm for rna inverse folding and molecular design. *Journal of bioinformatics and computational biology*, 11(02):1350001, 2013.
- Garcia-Martin, J. A., Dotu, I., and Clote, P. Rnaifold 2.0: a web server and software to design custom and rfam-based rna molecules. *Nucleic Acids Research*, 43(W1):W513–W521, 2015.
- Geisler, S. and Collier, J. Rna in unexpected places: long non-coding rna functions in diverse cellular contexts. *Nature reviews Molecular cell biology*, 14(11):699–712, 2013.
- Gilmer, J., Schoenholz, S. S., Riley, P. F., Vinyals, O., and Dahl, G. E. Neural message passing for quantum chemistry. In *International conference on machine learning*, pp. 1263–1272. PMLR, 2017.
- Gong, S., Zhang, C., and Zhang, Y. Rna-align: quick and accurate alignment of rna 3d structures based on size-independent tm-scoring. *Bioinformatics*, 35(21):4459–4461, 2019.
- Gstir, R., Schafferer, S., Scheideler, M., Misslinger, M., Griehl, M., Daschil, N., Humpel, C., Obermair, G. J., Schmuckermair, C., Striessnig, J., et al. Generation of a neuro-specific microarray reveals novel differentially expressed noncoding rnas in mouse models for neurodegenerative diseases. *Rna*, 20(12):1929–1943, 2014.
- Guo, P., Coban, O., Snead, N. M., Trebley, J., Hoepflich, S., Guo, S., and Shu, Y. Engineering rna for targeted sirna delivery and medical application. *Advanced drug delivery reviews*, 62(6):650–666, 2010.
- Hofacker, I. L. Vienna rna secondary structure server. *Nucleic acids research*, 31(13):3429–3431, 2003.
- Hofacker, I. L. Rna secondary structure analysis using the vienna rna package. *Current protocols in bioinformatics*, 26(1):12–2, 2009.
- Hofacker, I. L., Fontana, W., Stadler, P. F., Bonhoeffer, L. S., Tacker, M., and Schuster, P. Fast folding and comparison of rna secondary structures. *Monatshefte für Chemie/Chemical Monthly*, 125(2):167–188, 1994.
- Hsu, C., Verkuil, R., Liu, J., Lin, Z., Hie, B., Sercu, T., Lerer, A., and Rives, A. Learning inverse folding from millions of predicted structures. *bioRxiv*, 2022.
- Hu, B., Xia, J., Zheng, J., Tan, C., Huang, Y., Xu, Y., and Li, S. Z. Protein language models and structure prediction: Connection and progression, 2022.
- Ingraham, J., Garg, V., Barzilay, R., and Jaakkola, T. Generative models for graph-based protein design. *Advances in neural information processing systems*, 32, 2019.
- Jacobson, A. B. and Zuker, M. Structural analysis by energy dot plot of a large mrna. *Journal of molecular biology*, 233(2):261–269, 1993.
- Jeschek, M., Reuter, R., Heinisch, T., Trindler, C., Klehr, J., Panke, S., and Ward, T. R. Directed evolution of artificial metalloenzymes for in vivo metathesis. *Nature*, 537(7622):661–665, 2016.
- Jing, B., Eismann, S., Suriana, P., Townshend, R. J. L., and Dror, R. Learning from protein structure with geometric vector perceptrons. In *International Conference on Learning Representations*, 2020.
- Jumper, J., Evans, R., Pritzel, A., Green, T., Figurnov, M., Ronneberger, O., Tunyasuvunakool, K., Bates, R., Žídek, A., Potapenko, A., et al. Highly accurate protein structure prediction with alphafold. *Nature*, 596(7873):583–589, 2021.
- Kaushik, K., Sivadas, A., Vellarikkal, S. K., Verma, A., Jayarajan, R., Pandey, S., Sethi, T., Maiti, S., Scaria, V., and Sivasubbu, S. Rna secondary structure profiling in zebrafish reveals unique regulatory features. *BMC genomics*, 19(1):1–17, 2018.
- Kleinkauf, R., Houwaart, T., Backofen, R., and Mann, M. antarna–multi-objective inverse folding of pseudoknot rna using ant-colony optimization. *BMC bioinformatics*, 16(1):1–7, 2015a.

- Kleinkauf, R., Mann, M., and Backofen, R. antarna: ant colony-based rna sequence design. *Bioinformatics*, 31(19):3114–3121, 2015b.
- Knudsen, B. and Hein, J. Pfold: Rna secondary structure prediction using stochastic context-free grammars. *Nucleic acids research*, 31(13):3423–3428, 2003.
- Kortmann, J. and Narberhaus, F. Bacterial rna thermometers: molecular zippers and switches. *Nature reviews microbiology*, 10(4):255–265, 2012.
- Law, J. A. and Jacobsen, S. E. Establishing, maintaining and modifying dna methylation patterns in plants and animals. *Nature Reviews Genetics*, 11(3):204–220, 2010.
- Li, Z., Yang, Y., Faraggi, E., Zhan, J., and Zhou, Y. Direct prediction of profiles of sequences compatible with a protein structure by neural networks with fragment-based local and energy-based nonlocal profiles. *Proteins: Structure, Function, and Bioinformatics*, 82(10):2565–2573, 2014.
- Lorenz, R., Bernhart, S. H., Höner zu Siederdisen, C., Tafer, H., Flamm, C., Stadler, P. F., and Hofacker, I. L. Viennarna package 2.0. *Algorithms for molecular biology*, 6(1):1–14, 2011.
- Martell, J. D., Yamagata, M., Deerinck, T. J., Phan, S., Kwa, C. G., Ellisman, M. H., Sanes, J. R., and Ting, A. Y. A split horseradish peroxidase for the detection of intercellular protein–protein interactions and sensitive visualization of synapses. *Nature biotechnology*, 34(7):774–780, 2016.
- Mathews, D. H. Rna secondary structure analysis using rnastructure. *Current Protocols in Bioinformatics*, 46(1):12–6, 2014.
- Mathews, D. H., Disney, M. D., Childs, J. L., Schroeder, S. J., Zuker, M., and Turner, D. H. Incorporating chemical modification constraints into a dynamic programming algorithm for prediction of rna secondary structure. *Proceedings of the National Academy of Sciences*, 101(19):7287–7292, 2004.
- McCaskill, J. S. The equilibrium partition function and base pair binding probabilities for rna secondary structure. *Biopolymers: Original Research on Biomolecules*, 29(6-7):1105–1119, 1990.
- Meyer, S., Chappell, J., Sankar, S., Chew, R., and Lucks, J. B. Improving fold activation of small transcription activating rnas (stars) with rational rna engineering strategies. *Biotechnology and bioengineering*, 113(1):216–225, 2016.
- Miao, Z., Adamiak, R. W., Blanchet, M.-F., Boniecki, M., Bujnicki, J. M., Chen, S.-J., Cheng, C., Chojnowski, G., Chou, F.-C., Cordero, P., et al. Rna-puzzles round ii: assessment of rna structure prediction programs applied to three large rna structures. *Rna*, 21(6):1066–1084, 2015.
- Miao, Z., Adamiak, R. W., Antczak, M., Batey, R. T., Becka, A. J., Biesiada, M., Boniecki, M. J., Bujnicki, J. M., Chen, S.-J., Cheng, C. Y., et al. Rna-puzzles round iii: 3d rna structure prediction of five riboswitches and one ribozyme. *Rna*, 23(5):655–672, 2017.
- Miao, Z., Adamiak, R. W., Antczak, M., Boniecki, M. J., Bujnicki, J., Chen, S.-J., Cheng, C. Y., Cheng, Y., Chou, F.-C., Das, R., et al. Rna-puzzles round iv: 3d structure predictions of four ribozymes and two aptamers. *RNA*, 26(8):982–995, 2020.
- Nagamune, T. Biomolecular engineering for nanobio/bionanotechnology. *Nano convergence*, 4(1):1–56, 2017.
- Nicholas, R. and Zuker, M. Unafold: Software for nucleic acid folding and hybridization. *Bioinformatics*, 453:3–31, 2008.
- Noller, H. F. Structure of ribosomal rna. *Annual review of biochemistry*, 53(1):119–162, 1984.
- O’Connell, J., Li, Z., Hanson, J., Heffernan, R., Lyons, J., Paliwal, K., Dehzangi, A., Yang, Y., and Zhou, Y. Spin2: Predicting sequence profiles from protein structures using deep neural networks. *Proteins: Structure, Function, and Bioinformatics*, 86(6):629–633, 2018.
- Pearce, R., Omenn, G. S., and Zhang, Y. De novo rna tertiary structure prediction at atomic resolution using geometric potentials from deep learning. *bioRxiv*, 2022.
- Pugh, G. C., Burns, J. R., and Howorka, S. Comparing proteins and nucleic acids for next-generation biomolecular engineering. *Nature Reviews Chemistry*, 2(7):113–130, 2018.
- Qi, Y. and Zhang, J. Z. Denscpd: improving the accuracy of neural-network-based computational protein sequence design with densenet. *Journal of chemical information and modeling*, 60(3):1245–1252, 2020.
- Ramakrishnan, V. The ribosome emerges from a black box. *Cell*, 159(5):979–984, 2014.
- Retwitzer, M. D., Reinharz, V., Churkin, A., Ponty, Y., Waldispühl, J., and Barash, D. incarnablnv 2.0: a webserver and software with motif control for fragment-based design of rnas. *Bioinformatics*, 36(9):2920–2922, 2020.

- Rich, A. and RajBhandary, U. Transfer rna: molecular structure, sequence, and properties. *Annual review of biochemistry*, 45(1):805–860, 1976.
- Rose, P. W., Prlić, A., Altunkaya, A., Bi, C., Bradley, A. R., Christie, C. H., Costanzo, L. D., Duarte, J. M., Dutta, S., Feng, Z., et al. The rcsb protein data bank: integrative view of protein, gene and 3d structural information. *Nucleic acids research*, pp. gkw1000, 2016.
- Rosenbaum, L. Tragedy, perseverance, and chance—the story of car-t therapy. *N Engl J Med*, 377(14):1313–1315, 2017.
- Roth, A. and Breaker, R. R. The structural and functional diversity of metabolite-binding riboswitches. *Annual review of biochemistry*, 78:305, 2009.
- Runge, F., Stoll, D., Falkner, S., and Hutter, F. Learning to design rna. In *International Conference on Learning Representations*, 2018.
- Ryu, D. D. and Nam, D.-H. Recent progress in biomolecular engineering. *Biotechnology progress*, 16(1):2–16, 2000.
- Sato, K., Hamada, M., Asai, K., and Mituyama, T. Centroid-fold: a web server for rna secondary structure prediction. *Nucleic acids research*, 37(suppl_2):W277–W280, 2009.
- Shen, T., Hu, Z., Peng, Z., Chen, J., Xiong, P., Hong, L., Zheng, L., Wang, Y., King, I., Wang, S., et al. E2efold-3d: End-to-end deep learning method for accurate de novo rna 3d structure prediction. *arXiv preprint arXiv:2207.01586*, 2022.
- Singh, J., Hanson, J., Paliwal, K., and Zhou, Y. Rna secondary structure prediction using an ensemble of two-dimensional deep neural networks and transfer learning. *Nature communications*, 10(1):1–13, 2019.
- Singh, J., Paliwal, K., Singh, J., and Zhou, Y. Rna backbone torsion and pseudotorsion angle prediction using dilated convolutional neural networks. *Journal of Chemical Information and Modeling*, 61(6):2610–2622, 2021.
- Sloma, M. F. and Mathews, D. H. Exact calculation of loop formation probability identifies folding motifs in rna secondary structures. *RNA*, 22(12):1808–1818, 2016.
- Strokach, A., Becerra, D., Corbi-Verge, C., Perez-Riba, A., and Kim, P. M. Fast and flexible protein design using deep graph neural networks. *Cell systems*, 11(4):402–411, 2020.
- Tan, C., Xia, J., Wu, L., and Li, S. Z. Co-learning: Learning from noisy labels with self-supervision. In *Proceedings of the 29th ACM International Conference on Multimedia*, pp. 1405–1413, 2021.
- Tan, C., Gao, Z., Li, S., Xu, Y., and Li, S. Z. Temporal attention unit: Towards efficient spatiotemporal predictive learning. *arXiv preprint arXiv:2206.12126*, 2022a.
- Tan, C., Gao, Z., and Li, S. Z. Rfold: Towards simple yet effective rna secondary structure prediction. *arXiv preprint arXiv:2212.14041*, 2022b.
- Tan, C., Gao, Z., and Li, S. Z. Simvp: Towards simple yet powerful spatiotemporal predictive learning. *arXiv preprint arXiv:2211.12509*, 2022c.
- Tan, C., Gao, Z., and Li, S. Z. Target-aware molecular graph generation. *arXiv preprint arXiv:2202.04829*, 2022d.
- Tan, C., Gao, Z., Wu, L., Li, S., and Li, S. Z. Hyperspherical consistency regularization. In *Proceedings of the IEEE/CVF Conference on Computer Vision and Pattern Recognition*, pp. 7244–7255, 2022e.
- Tan, C., Gao, Z., Xia, J., and Li, S. Z. Generative de novo protein design with global context. *arXiv preprint arXiv:2204.10673*, 2022f.
- Townshend, R. J., Eismann, S., Watkins, A. M., Rangan, R., Karelina, M., Das, R., and Dror, R. O. Geometric deep learning of rna structure. *Science*, 373(6558):1047–1051, 2021.
- Vandivier, L. E., Anderson, S. J., Foley, S. W., and Gregory, B. D. The conservation and function of rna secondary structure in plants. *Annual review of plant biology*, 67: 463, 2016.
- Vaswani, A., Shazeer, N., Parmar, N., Uszkoreit, J., Jones, L., Gomez, A. N., Kaiser, L., and Polosukhin, I. Attention is all you need. *Advances in neural information processing systems*, 30, 2017.
- Wachsmuth, M., Findeiß, S., Weissheimer, N., Stadler, P. F., and Mörl, M. De novo design of a synthetic riboswitch that regulates transcription termination. *Nucleic acids research*, 41(4):2541–2551, 2013.
- Wang, J., Cao, H., Zhang, J. Z., and Qi, Y. Computational protein design with deep learning neural networks. *Scientific reports*, 8(1):1–9, 2018.
- Wanrooij, P. H., Uhler, J. P., Simonsson, T., Falkenberg, M., and Gustafsson, C. M. G-quadruplex structures in rna stimulate mitochondrial transcription termination and primer formation. *Proceedings of the National Academy of Sciences*, 107(37):16072–16077, 2010.
- Warner, K. D., Hajdin, C. E., and Weeks, K. M. Principles for targeting rna with drug-like small molecules. *Nature reviews Drug discovery*, 17(8):547–558, 2018.

- Xiong, P., Wu, R., Zhan, J., and Zhou, Y. Pairing a high-resolution statistical potential with a nucleobase-centric sampling algorithm for improving rna model refinement. *Nature communications*, 12(1):1–11, 2021.
- Yang, X., Yoshizoe, K., Taneda, A., and Tsuda, K. Rna inverse folding using monte carlo tree search. *BMC bioinformatics*, 18(1):1–12, 2017.
- Zadeh, J. N., Steenberg, C. D., Bois, J. S., Wolfe, B. R., Pierce, M. B., Khan, A. R., Dirks, R. M., and Pierce, N. A. Nupack: Analysis and design of nucleic acid systems. *Journal of computational chemistry*, 32(1):170–173, 2011a.
- Zadeh, J. N., Wolfe, B. R., and Pierce, N. A. Nucleic acid sequence design via efficient ensemble defect optimization. *Journal of computational chemistry*, 32(3):439–452, 2011b.
- Zhang, Y. and Skolnick, J. Scoring function for automated assessment of protein structure template quality. *Proteins: Structure, Function, and Bioinformatics*, 57(4):702–710, 2004.
- Zhang, Y. and Skolnick, J. Tm-align: a protein structure alignment algorithm based on the tm-score. *Nucleic acids research*, 33(7):2302–2309, 2005.
- Zhang, Y., Chen, Y., Wang, C., Lo, C.-C., Liu, X., Wu, W., and Zhang, J. Prodcnn: Protein design using a convolutional neural network. *Proteins: Structure, Function, and Bioinformatics*, 88(7):819–829, 2020.
- Zheng, J., Li, S., Tan, C., Wu, C., Chen, Y., and Li, S. Z. Leveraging graph-based cross-modal information fusion for neural sign language translation. *arXiv preprint arXiv:2211.00526*, 2022.
- Zuker, M. Mfold web server for nucleic acid folding and hybridization prediction. *Nucleic acids research*, 31(13):3406–3415, 2003.